


Article

Steady-State Shear Rheology of Aqueous Noncolloidal Carbonate Suspensions

William Apau Marfo¹, Kristofer Gunnar Paso²  and Maarten Felix^{1,*}

¹ Department of Geosciences, Norwegian University of Science and Technology, 7031 Trondheim, Norway; williaam@stud.ntnu.no

² Department of Chemical Engineering, Norwegian University of Science and Technology, 7491 Trondheim, Norway; kristofer.g.paso@ntnu.no

* Correspondence: maarten.felix@ntnu.no

Abstract: Carbonate muds are essential sedimentary components in geological carbon cycles. Model carbonate muds are prepared from crushed, sieved carbonate rock. The carbonate rock particles are primarily smaller than 62.5 μm . Steady-state shear viscosity was measured for model carbonate muds prepared from three types of carbonate rock: limestone Grey, limestone Marl, and limestone Castleton. Model carbonate muds were prepared using fresh water or 3.5 g/L NaCl solution. The carbonate particle concentrations were 1.81 volume percent and 26.95 volume percent, representing semi-dilute and concentrated particle regimes, respectively. Carbonate mud viscosity was measured at temperatures ranging from 8 °C to 35 °C. Shear rates ranged from 60 s^{-1} to 2500 s^{-1} . Pseudoplasticity occurs at low shear rates and is caused by the release of occluded water during shear-driven breakup and dispersal of particle aggregates. Shear thickening occurs at high shear rates and is caused by transient particle clusters, called hydroclusters, that are reinforced by lubrication forces or frictional particle contacts. Carbonate mud viscosity decreases at increasing temperatures. The presence of 3.5 g/L NaCl in the aqueous phase slightly increased the mud viscosity in the semi-dilute particle concentration regime because of a weak viscosifying effect of NaCl on the aqueous phase. In the concentrated particle regime, electrolytes screened electroviscous effects, reducing the viscosity of muds containing particles with electrically charged surfaces. In aqueous solution, limestone Marl had a comparatively high concentration of charged particles on its surface. Limestone Castleton had a comparatively low concentration of charged particles on its surface. Surface charges were not rheologically evident on limestone Grey.

Keywords: carbonate mud; rheology; shear thinning; shear thickening; noncolloidal suspension; electroviscous effects; hydroclusters; pseudoplasticity; limestone; aggregation



Citation: Marfo, W.A.; Paso, K.G.; Felix, M. Steady-State Shear Rheology of Aqueous Noncolloidal Carbonate Suspensions. *Geosciences* **2024**, *14*, 232. <https://doi.org/10.3390/geosciences14090232>

Academic Editor: José Manuel Castro

Received: 9 July 2024

Revised: 19 August 2024

Accepted: 27 August 2024

Published: 29 August 2024



Copyright: © 2024 by the authors. Licensee MDPI, Basel, Switzerland. This article is an open access article distributed under the terms and conditions of the Creative Commons Attribution (CC BY) license (<https://creativecommons.org/licenses/by/4.0/>).

1. Introduction

1.1. Carbonate Muds

Natural carbonate muds are aqueous dispersions of fine-grained carbonate particles. Carbonate muds may also contain ions, dissolved gases, nutrients, microorganisms, trace elements, extraneous phosphates, organic material, and extraneous or detrital minerals such as siliciclastics. The primary mineral components of carbonate mud are calcite and aragonite. Carbonate muds are predominantly deposited in low-energy geological systems [1], such as reefs, back reefs, protected marine bays, sabkhas, shallow shelves, deep marine basins, tidal flats, and lagoons.

Carbonate mud constitutes a significant sedimentary component in present-day carbonate environments and the historical carbonate rock record. Carbonate muds play a substantial role as a primary sink in the geological carbon cycle [1–3]. Despite being commonly found and economically significant, carbonate rocks are not well understood in comparison to other types of sedimentary rock, such as siliciclastics. Carbonate mud has

been debated to originate from two distinct mechanisms: (1) the precipitation of unstable aragonites which nucleate and crystallize into an orthorhombic crystal structure, resulting in the formation of suspended carbonate particles, and (2) the breakdown and scattering of calcifying microorganisms, including algae and foraminifera, into mud-sized carbonate particles. Trower et al. [2] argue that the mechanisms mentioned above conflict with geochemical observations of modern carbonate mud. They conclude that abrasion of carbonate sand-sized particles during transport generates significant carbonate muds at rates two to three orders of magnitude faster than the rates predicted for the two mechanisms listed above. Geymen et al. [3], however, argue that the abrasion of carbonate sand-sized particles and the breakdown of algae cannot generate carbonate mud and that, instead, carbonate mud is sourced from aragonite precipitated from seawater at high alkalinity.

1.2. Noncolloidal Suspension Rheology

Unlike siliciclastic mud, research on carbonate mud is limited, and its rheological properties have not been thoroughly investigated. The first study on carbonate mud was conducted by Alince and Lepoutre [4], who investigated the rheological behavior of carbonate mud. They investigated the shear-thickening behavior of concentrated carbonate suspensions and concluded that introducing a second particle of a different size reduces the severity of shear thickening, thus reducing the viscosity of the suspension and increasing the critical shear rate. Another experiment by Schieber et al. [1] revealed that carbonate muds are cohesive and can form floccules below a certain critical velocity and that the migration of the ripples leads to the formation of accreted mud beds. However, the experiment did not explain the intermolecular forces causing the cohesion between the particles, and the rheological properties of carbonate mud were overlooked.

Noncolloidal suspensions often show pseudoplasticity at low shear rates and shear thickening at high shear rates [5]. The mechanisms of pseudoplasticity are not completely understood, especially for noncolloidal suspensions with polydisperse particle sizes. At quiescence, thermal forces cause noninteracting particles to adopt disorganized spatial arrangements. At increasing shear rates, noninteracting particles rearrange and align in the direction of flow. Rearrangement and alignment of noninteracting particles in the flow direction occurs in conjunction with shear thinning. The primary shear-thinning mechanism of noninteracting particles is commonly considered to be particle rearrangement and alignment. However, particle aggregation further complicates the understanding of pseudoplasticity in noncolloidal suspensions.

Interparticle interactions may also cause shear thinning in suspensions. Interparticle attractions often cause aggregation. Aggregation entails fluid occlusion in the aggregates. Occluded fluid is effectively immobilized within particle aggregates. Occluded fluid is largely shielded from macroscopic shear forces. From the perspective of steady-state rheology, occluded fluid is a constituent part of the effective dispersed phase of a suspension. In quantitative rheological correlations, occluded fluid contributes directly to the effective dispersed-phase volume fraction of a solid suspension. In shearing fields, relative fluid motion induced by the velocity gradient results in persistent deformation and separation of fluid elements. Persistent deformation and separation of fluid elements results in the exertion of extensional stresses on particles or aggregates dispersed within a shearing field. Extensional stresses scale with shear rates. At sufficiently high shear rates, extensional stresses break apart large aggregates into smaller aggregates and separate individual particles from aggregates. The process of disaggregation releases occluded water to the bulk aqueous continuous phase. The release of occluded water to the bulk aqueous continuous phase reduces the effective dispersed-phase volume fraction of a suspension. Consequently, the suspension viscosity decreases. Shearing-induced disaggregation is a separate and distinct mechanism of shear thinning in suspensions and may supplement the primary shear-thinning mechanism related to particle rearrangement and alignment.

The intensity of shear thickening depends on the size, shape, and volume fraction of particles. Weak shear thickening may occur at low particle volume fractions, as ob-

served in starch suspensions. Weak shear thickening is characterized as a continuous increase in viscosity as the shear rate increases. Strong shear thickening may occur at high particle volume fractions and is often marked by a sudden, discontinuous increase in viscosity as the shear rate increases. Shear thickening is caused by the formation of transient particle clusters, known as hydroclusters, that are reinforced by short-range interparticle interactions such as lubrication forces and frictional particle contacts. Within each hydrocluster, relative translational motion of individual particles is temporarily restricted by lubrication forces or frictional particle contacts [6], temporarily occluding or immobilizing both particles and fluid within the hydrocluster. The entire hydrocluster becomes a temporary constituent portion of the effective dispersed phase of a suspension due to fluid occlusion. Quantitatively, the presence of a hydrocluster causes a temporary increase in the effective dispersed phase volume fraction of a fluid. Integrated over a macroscopic fluid volume, the presence of hydroclusters causes a persistent increase in the effective dispersed phase volume fraction of a suspension. Consequently, the suspension viscosity increases. Shear thickening is a ubiquitous rheological feature of concentrated colloids and suspensions. Semi-dilute noncolloidal suspensions are also known to shear-thicken. For example, semi-dilute noncolloidal starch suspensions exhibit shear-thickening rheology [7].

Compiled rheological data of diverse concentrated colloidal and suspension systems, encompassing particle sizes ranging from 10 nm to 100 μm , demonstrate that the critical shear rate at the onset of shear thickening decreases with increasing particle size, with an inverse quadratic mathematical dependency [8]. In general, suspensions of large particles commence shear thickening at substantially lower shear rates than suspensions of small particles. For noncolloidal suspensions, the comparatively large particle size implies that shear thickening can be expected to occur over wide ranges of shear rates.

1.3. Model Carbonate Muds

In the current investigation, model carbonate muds were prepared to emulate the essential characteristics and features of real carbonate muds in nature. The carbonate rocks were obtained from various sources. The carbonate rocks were crushed and sieved to yield fine carbonate particles, smaller than 62.5 μm . Subsequently, the carbonate particles were dispersed in either fresh water or an aqueous NaCl solution. The steady-state shear rheology of the model carbonate mud suspensions was investigated for various carbonate types, particle concentrations, and temperature conditions. In addition, the determination of rheological properties was performed using two different continuous-phase fluids: (1) fresh water and (2) aqueous NaCl solution (to emulate saline water conditions in transport systems). Steady-state shear rheology reveals insights into interparticle interactions in carbonate mud suspensions. The use of model carbonate muds effectively circumvents experimental artifacts arising from the presence of noncarbonate material which is often present in carbonate muds found in natural environments, but obscures measurement and interpretation of rheological behavior. The presence of noncarbonate material complicates experimental investigation of interparticle interactions and fluid rheology by producing experimental artifacts and extraneous, interfering instrumental signals. Exclusion of non-carbonate solid material from the investigation enables granular interactions between carbonate particles to be emulated in a representative aqueous environment and probed using bulk rheological methods. Usage of well-defined carbonate mud enables rheometric signals to be interpreted directly in the context of interfacial phenomena and interparticle interactions. Use of defined-composition suspensions implies that the particles remain unsettled. A distinct disadvantage of using unsettled model carbonate mud dispersions for rheological measurements is that gravitational stability remains unconfirmed. Depending on the selected particle concentration regime, a given model carbonate mud suspension may be either representative of carbonate particles undergoing sedimentation in a water column or, alternatively, representative of settled carbonate mud deposits found in sediments.

The motivation of the current investigation was not to accurately emulate the detailed fluid composition or particle packing conditions of geological carbonate mud sediments.

Instead, in the current investigation, carbonate particles were first subjected to strong shear forces to uniformly disperse the particles in the aqueous phase at defined concentrations. Subsequently, rheological measurements were performed to reveal insights into the physical nature of interparticle interactions and steady-state flow dynamics. The probed interparticle interactions and rheological dynamics are expected to extend broadly to both settling and settled carbonate particle dispersions.

1.4. Testing Matrix

A dedicated testing matrix was used to thoroughly investigate the rheological properties of the model carbonate muds. A thorough rheological testing regimen was performed with limestone Marl and limestone Grey suspensions, which had completely different surface electric properties. Specifically, rheological tests were performed with limestone Marl and limestone Grey muds at particle concentrations denoted as 50 g/1 L, defined as 50 g of particles added to each liter of water, and denoted as 25 g/25 mL, defined as 25 g of particles added to each 25 mL of water. Limited rheological tests were performed with model carbonate muds prepared with limestone Castleton, which has intermediate surface electric properties compared to limestone Marl and limestone Grey muds. Due to its having intermediate surface electric properties, a complete rheological characterization was not necessary for the limestone Castleton muds. Hence, rheological tests were performed with limestone Castleton muds only at particle concentrations denoted as 25 g/25 mL.

Rheological measurements were performed on model carbonate muds prepared with freshwater or a saline solution. The saline solution consisted of 3.5 g of NaCl per liter, emulating the average salinity of the Earth’s oceans. Measurement temperatures were selected in the range of 8 °C to 35 °C, reflecting a variety of liquid thermal conditions for water at atmospheric pressure.

The rheologically applied shear rates ranged from 60 s⁻¹ to 2500 s⁻¹. Carbonate suspensions are gravitationally unstable. However, semi-dilute carbonate muds are more susceptible to gravitational settling than concentrated carbonate muds at low shear rates. For semi-dilute muds, shear rates less than 300 s⁻¹ enable gravitational settling. Semi-dilute muds are much more susceptible to inertially driven secondary and transition flows at high shear rates because of an elevated Reynolds number. Hence, for semi-dilute carbonate suspensions, a shear rate range of 300 s⁻¹ to 1500 s⁻¹ was applied, ensuring gravitational stability while circumventing inertially driven secondary and transition flows in the measuring geometry. Table 1 shows the testing matrix.

Table 1. Experimental design, including the shear rate regimes.

Carbonate Particle Type	Temperature	Freshwater 50 g/1 L	Saline 50 g/1 L	Freshwater 25 g/25 mL	Saline 25 g/25 mL
Limestone Marl	8 °C	300 s ⁻¹ to 1500 s ⁻¹	300 s ⁻¹ to 1500 s ⁻¹	60 s ⁻¹ to 2500 s ⁻¹	60 s ⁻¹ to 2500 s ⁻¹
	20 °C	300 s ⁻¹ to 1500 s ⁻¹	300 s ⁻¹ to 1500 s ⁻¹	60 s ⁻¹ to 2500 s ⁻¹	60 s ⁻¹ to 2500 s ⁻¹
	30 °C	300 s ⁻¹ to 1500 s ⁻¹	300 s ⁻¹ to 1500 s ⁻¹	-	-
	35 °C	-	-	60 s ⁻¹ to 2500 s ⁻¹	60 s ⁻¹ to 2500 s ⁻¹
Limestone Castleton	8 °C	-	-	60 s ⁻¹ to 2500 s ⁻¹	60 s ⁻¹ to 2500 s ⁻¹
	20 °C	-	-	60 s ⁻¹ to 2500 s ⁻¹	60 s ⁻¹ to 2500 s ⁻¹
	35 °C	-	-	60 s ⁻¹ to 2500 s ⁻¹	60 s ⁻¹ to 2500 s ⁻¹
Limestone Grey	8 °C	300 s ⁻¹ to 1500 s ⁻¹	300 s ⁻¹ to 1500 s ⁻¹	60 s ⁻¹ to 2500 s ⁻¹	60 s ⁻¹ to 2500 s ⁻¹
	20 °C	300 s ⁻¹ to 1500 s ⁻¹	300 s ⁻¹ to 1500 s ⁻¹	60 s ⁻¹ to 2500 s ⁻¹	60 s ⁻¹ to 2500 s ⁻¹
	30 °C	300 s ⁻¹ to 1500 s ⁻¹	300 s ⁻¹ to 1500 s ⁻¹	-	-
	35 °C	-	-	60 s ⁻¹ to 2500 s ⁻¹	60 s ⁻¹ to 2500 s ⁻¹

2. Materials and Methods

2.1. Model Carbonate Mud Preparation

Carbonate mud suspensions were prepared from three different carbonate rock samples obtained from Castleton (limestone Castleton), Manchester (limestone Grey), and Mitcham (limestone Marl) in the United Kingdom (UK). The rock samples were initially crushed using a jaw crusher and subsequently reduced to finer particles using a disk mill and a planetary mill. The milled samples were then passed through a 62.5 μm sieve to obtain very fine limestone powder samples. The carbonate mud was prepared based on two different approaches. First, carbonate mud was prepared from all three carbonate samples using fresh and saline water (35 g of NaCl per liter). Semi-dilute carbonate mud samples were prepared by mixing 50 g of limestone powder for each 1 L of fresh or saline water. The semi-dilute carbonate mud sample concentrations are therefore denoted as 50 g/1 L. The same procedure was used to prepare concentrated carbonate mud samples. Concentrated carbonate mud samples were prepared by mixing 25 g of limestone powder for each 25 mL of fresh or saline water. The concentrated carbonate mud sample concentrations are therefore denoted as 25 g/25 mL. The two different mud preparation approaches were adopted to help simulate the behavior of carbonate mud in natural environments, the former representing low-concentration sediment flow and the latter representing high-concentration sediment flow. The introduction of saline water was to examine the influence of electrolytes (NaCl) on carbonate mud rheology.

The density of the limestone rock was 2.71 g per cubic centimeter. The carbonate muds denoted 50 g/1 L (both freshwater and saline) contained a 1.81% volume fraction of particles, representing the semi-dilute particle concentration regime, where interactions between particles were largely hydrodynamic in nature. The carbonate muds denoted 25 g/25 mL (both freshwater and saline) contained a 26.95% volume fraction of particles, representing the concentrated particle regime, where significant interparticle interactions occurred.

2.2. Rheometric Protocol

An Anton Paar rheometer, equipped with a concentric cylinder geometry (17 mm inner cylinder diameter and 18.44 mm outer diameter), was used to investigate the rheology of the carbonate muds at different temperatures. Prior to the viscosity and shear stress measurements, the carbonate mud suspensions were sheared at a rate of 2500 s^{-1} for 20 s to ensure complete suspension of the particles. Viscosity and shear stress data were obtained by using a prescribed shear rate ramp setting: 60 s^{-1} to 2500 s^{-1} for concentrated suspensions and 300 s^{-1} to 1500 s^{-1} for semi-dilute suspensions. The 50 g/1 L carbonate suspensions were sheared at a constant shear rate for 20 s before measurements were recorded for 10 data points. However, the 25 g/25 mL concentration carbonate suspensions were sheared at a constant shear rate for 20 s before measurements were recorded for 20 data points. To further understand the behavior of carbonate mud in natural environments, specific temperatures (from 8 to 35 degrees Celsius) were established during the rheometric measurements using the Anton Paar Physica rheometer.

2.3. Measurement of Particle Size Distributions

Particle size distribution analysis of the three particle samples was performed with a Mastersizer 3000, which operates on the principle of laser light scattering. A folded optical design enables a wide particle size range from 10 nm to 3.5 mm, utilizing a single optical path for measurement. A sequential combination of red- and blue-colored light sources was used for analysis to extend the measurement to apply to a wide particle size range. The particle size analysis was performed using the Mie and Fraunhofer scattering theories.

3. Results

3.1. The 50 g/1 L Carbonate Concentration

The flow curves of limestone Grey and limestone Marl muds at the denoted 50 g/1 L concentration are shown in Figure 1 for various temperature and salinity conditions. The

measured viscosity values for limestone Grey and limestone Marl muds at the denoted 50 g/1 L concentration are shown in Figure 2 for various temperature and salinity conditions. The model carbonate mud exhibits non-Newtonian behavior. An increase in shear rate causes a nonlinear increase in shear stress, highlighting the complex nature of carbonate mud's rheological response to mechanical forces. The observed trend of increasing shear stress with increasing shear rate occurs in freshwater and saline suspensions. Freshwater suspensions have slightly lower shear stress and viscosity values in comparison to saline suspensions. The slight, quantifiable disparity in rheological properties between the freshwater and saline mud suspensions is attributed to a weak viscosifying effect of NaCl on the aqueous phase. In the denoted 50 g/1 L concentration muds, viscosity increases with shear rate from 300 s^{-1} to 1500 s^{-1} , which is consistent with a relatively low shear rate onset for the shear thickening regime for the noncolloidal mud suspensions, consistent with theoretical considerations pertaining to the particle size dependence of the onset shear rate for shear thickening.

The viscosity increases in a relatively linear fashion with respect to the applied shear rate from 600 s^{-1} to 1500 s^{-1} . In other semi-dilute noncolloidal suspensions, such as corn starch suspensions, shear thickening occurs over broad ranges of shear rates [7]. The shear thickening observed in the semi-dilute noncolloidal model carbonate mud suspensions is consistent with the rheology of similar noncolloidal suspensions.

Figure 3 shows a comparative overlay of measured flow curves for limestone Grey and limestone Marl suspensions at a denoted 50 g/1 L concentration. The shear stress trends are remarkably similar for the limestone Grey and limestone Marl suspensions. Figure 4 shows a comparative overlay of measured viscosity values for limestone Grey and limestone Marl suspensions at a denoted 50 g/1 L concentration. The measured viscosity values are remarkably similar for the limestone Grey and limestone Marl suspensions.

Figure 5 shows flow curves at various temperatures for limestone Grey and limestone Marl suspensions at a denoted 50 g/1 L concentration. The measured shear stress values decrease with increasing temperature. Figure 6 shows viscosity values of the limestone Grey and limestone Marl suspensions at various temperatures at a denoted 50 g/1 L concentration. The measured viscosity values decrease with increasing temperature.

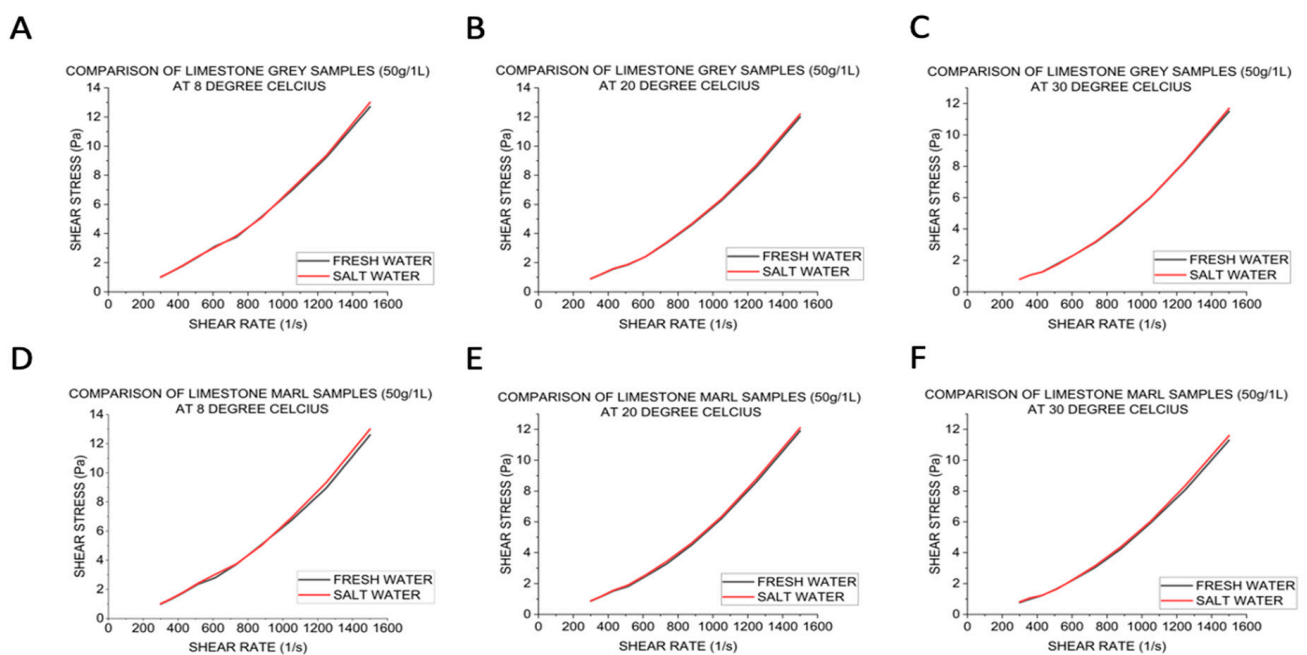


Figure 1. Influence of salinity on shear stress of 50 g/1 L concentration limestone Grey and limestone Marl suspensions.

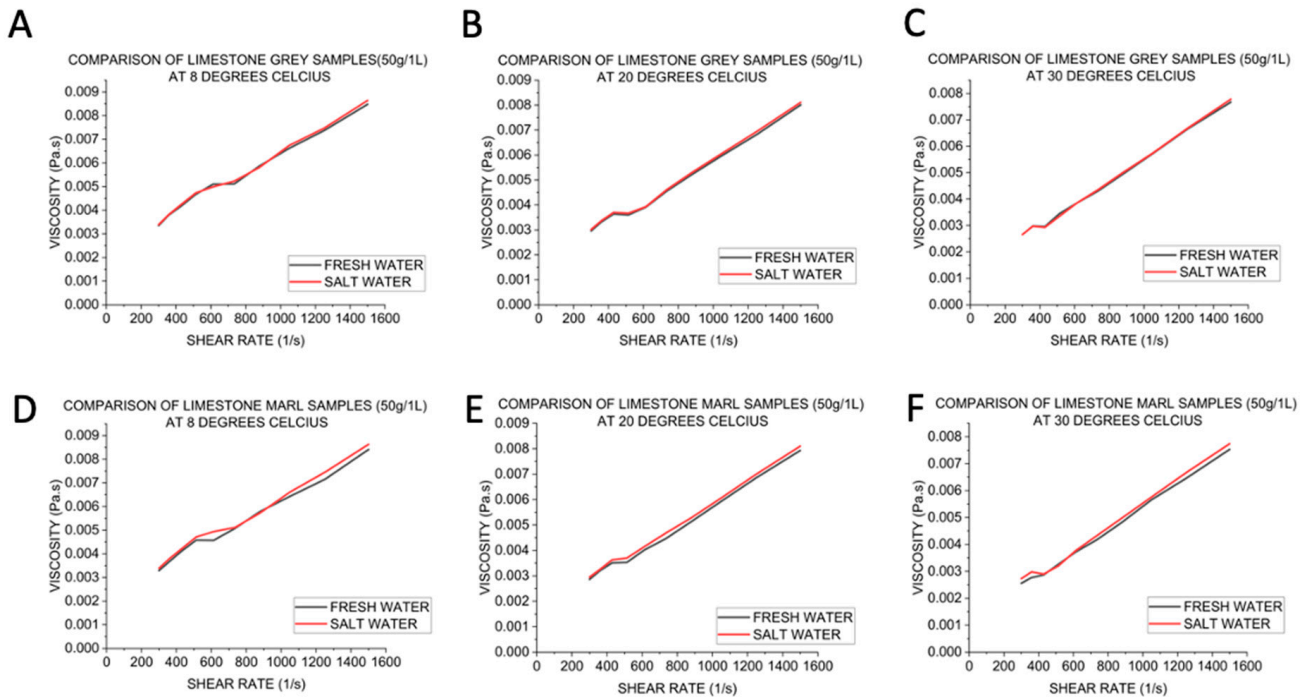


Figure 2. Influence of salinity on viscosity of 50 g/1 L concentration limestone Grey and limestone Marl suspensions.

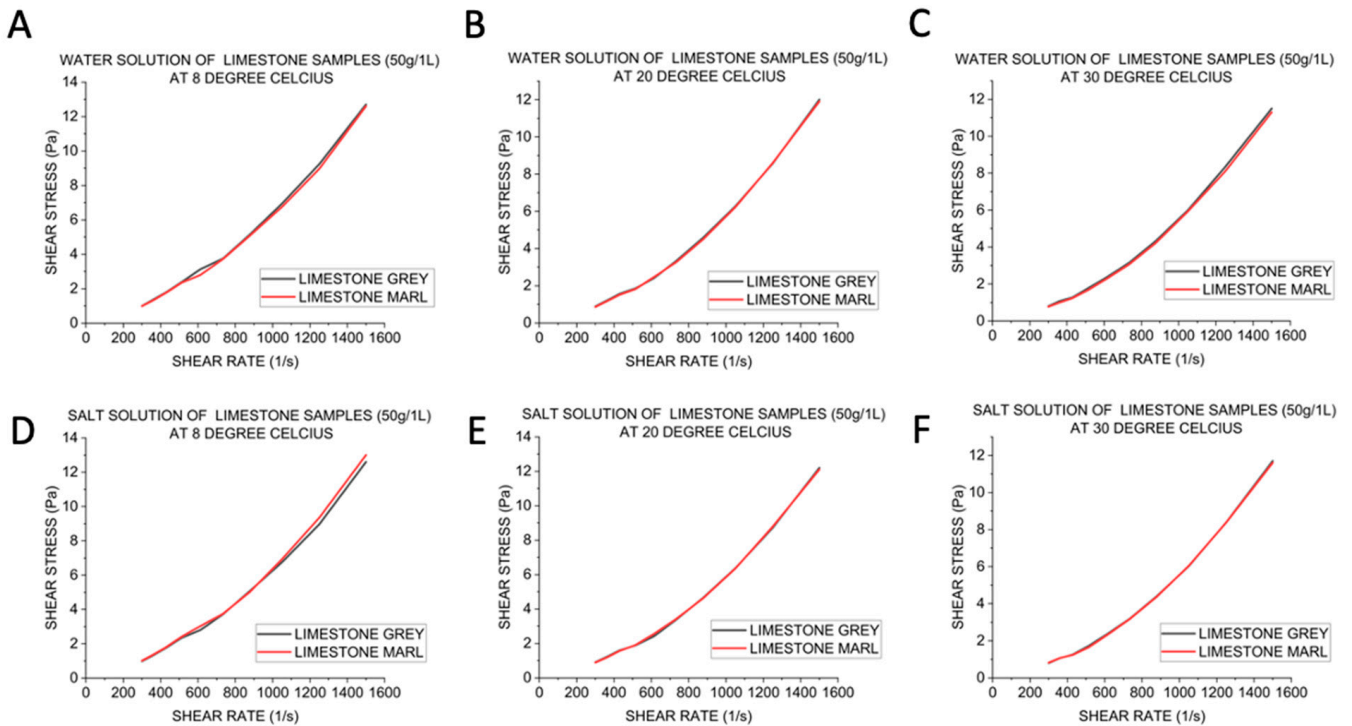


Figure 3. Influence of carbonate type on shear stress of 50 g/1 L concentration muds.

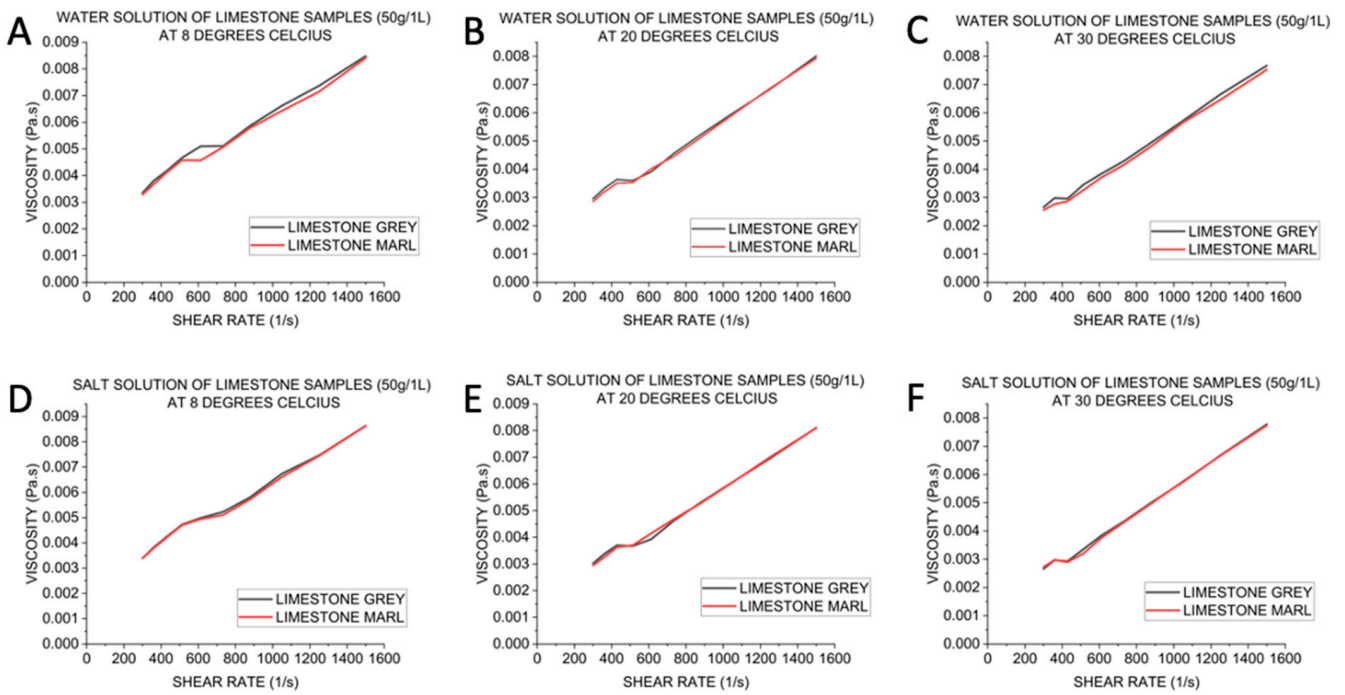


Figure 4. Influence of carbonate type on viscosity of 50 g/1 L concentration muds.

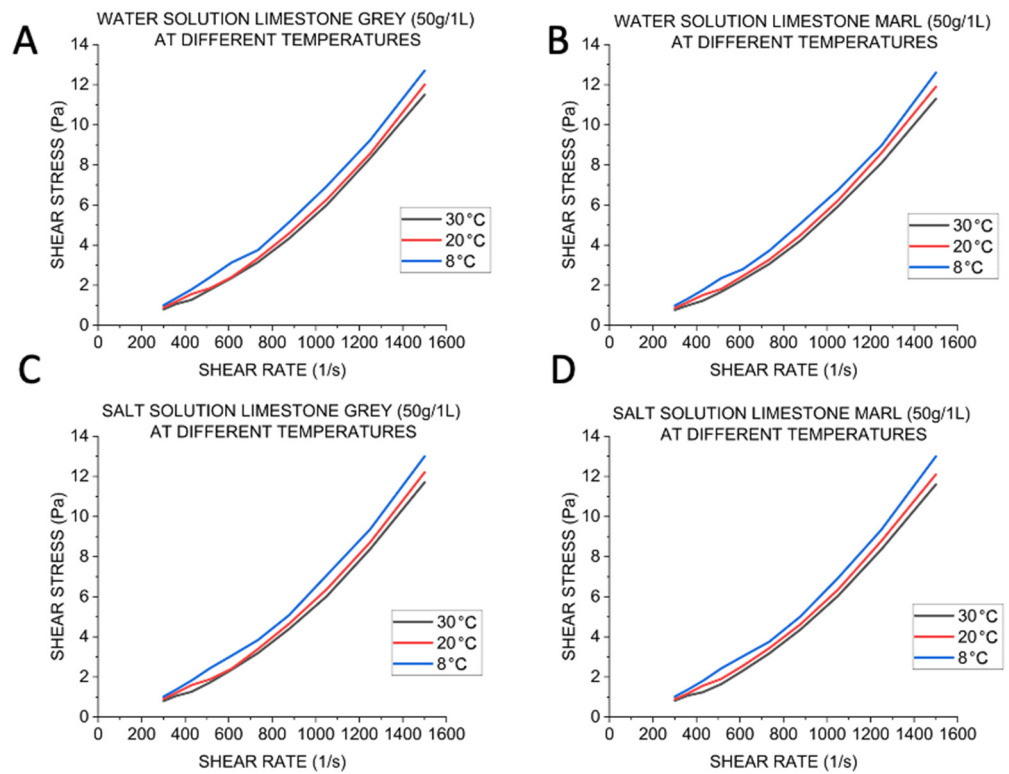


Figure 5. Influence of temperature on shear stress of 50 g/1 L concentration muds.

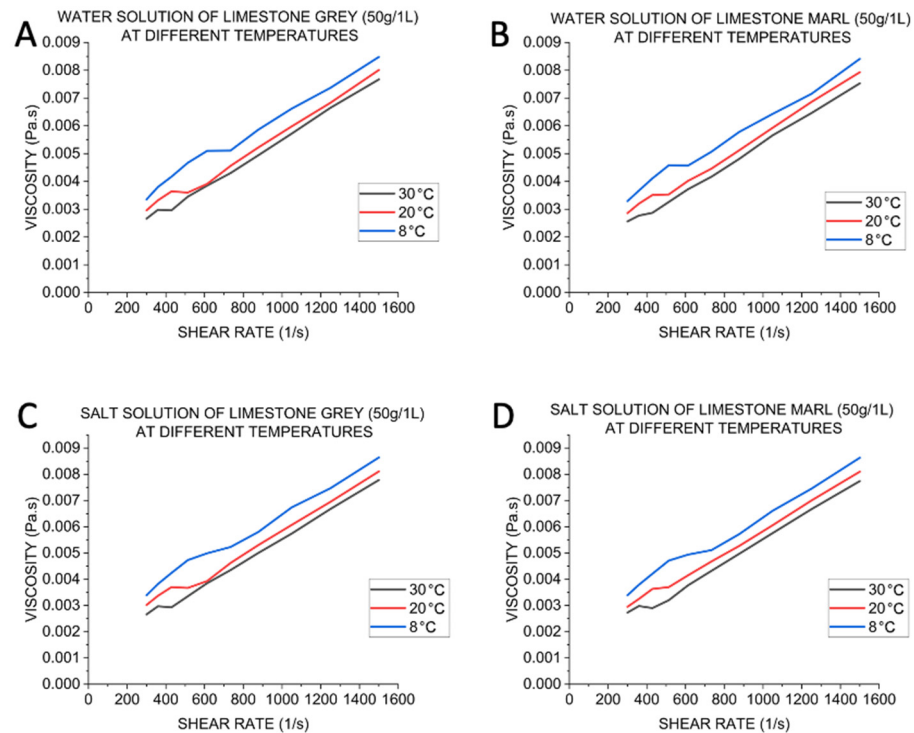


Figure 6. Influence of temperature on viscosity of 50 g/1 L concentration muds.

3.2. The 25 g/25 mL Concentration of Carbonates

Flow curves and viscosity values of the denoted 25 g/25 mL concentration limestone muds are shown in Figures 7 and 8, respectively. Individual plots in Figures 7 and 8 show a comparative overlay of rheological trends for model muds prepared with freshwater and saline solutions. Shear-thinning and shear-thickening regimes are evident in Figure 8. In the shear-thickening regime, viscosity values increase in a relatively linear fashion with respect to shear rate.

The rheological data shown in Figures 7 and 8 show revealing trends with respect to the presence of NaCl in the aqueous phase. For limestone Grey muds, the presence of NaCl in the aqueous phase had a very limited effect on the measured rheological parameters. For limestone Grey muds, shear stress trends were very similar for samples prepared with freshwater and saline solution. The measured viscosity values were very similar for limestone Grey muds prepared with freshwater and saline solution.

For limestone Marl muds, the presence of NaCl in the aqueous phase had a distinct influence on measured shear stress and viscosity values, especially in the shear-thinning regime and in the proximity of the onset of the shear-thickening regime. For limestone Marl muds, the presence of NaCl in the aqueous phase reduced shear stress and viscosity values over the entire measured range of shear rates.

For limestone Castleton muds, the presence of NaCl in the aqueous phase resulted in a slight reduction in viscosity in the shear-thinning regime, as shown in Figure 8. In the shear-thickening regime, shear stress values were very similar for Castleton muds prepared with freshwater and saline solutions. In the shear-thickening regime, viscosity values were very similar for Castleton muds prepared with freshwater and saline solutions.

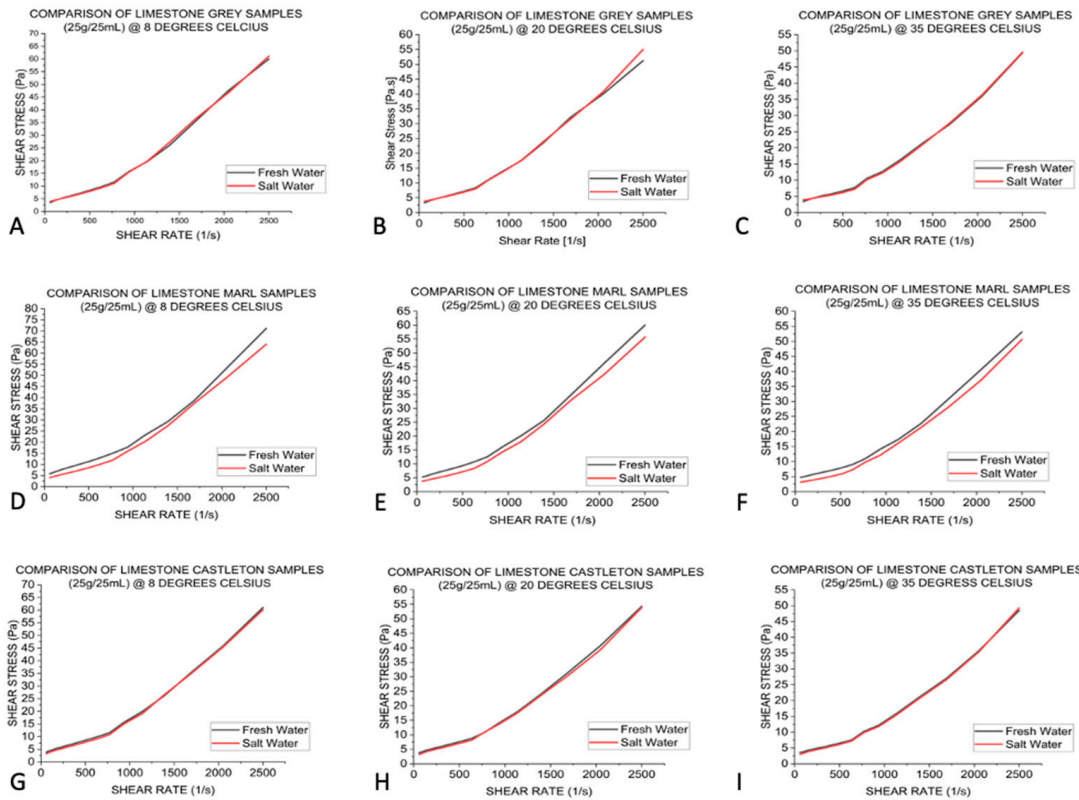


Figure 7. Influence of salinity on shear stress of 25 g/25 mL concentration muds.

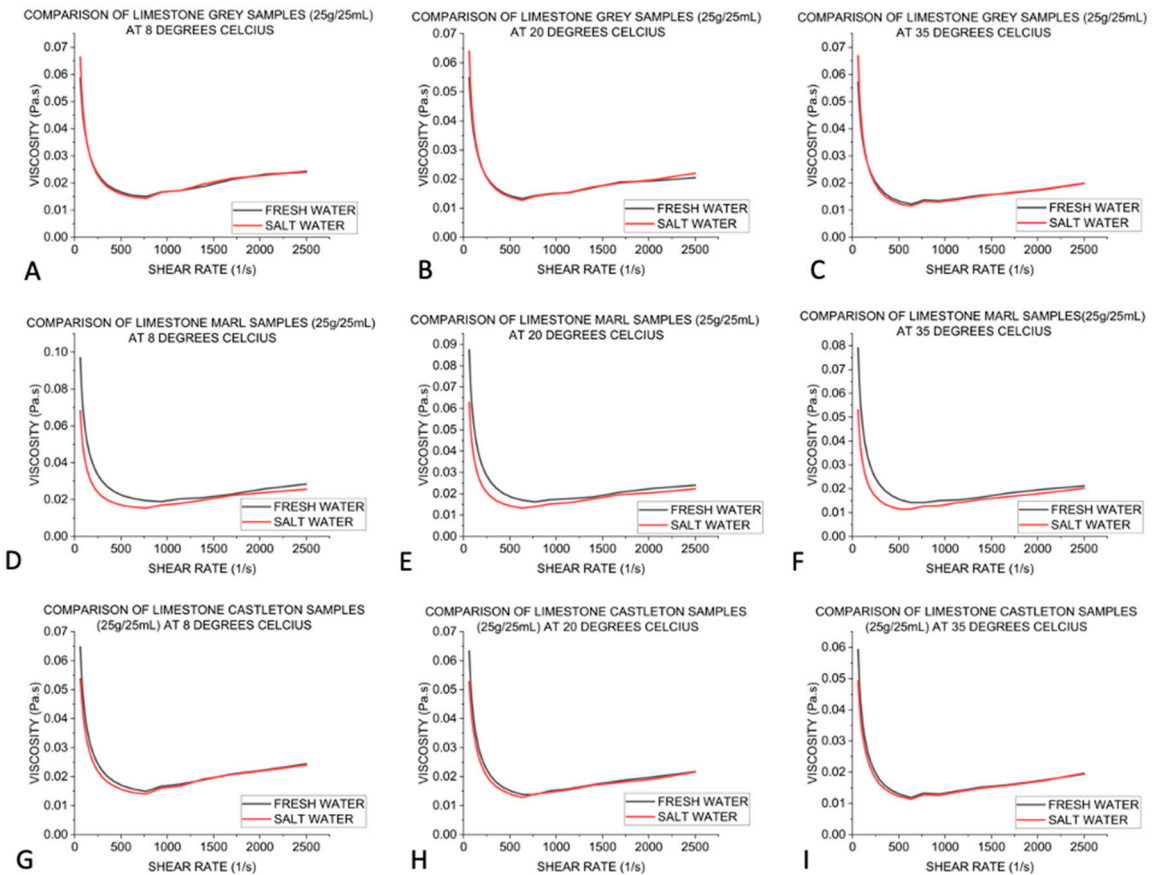


Figure 8. Influence of salinity on viscosity of 25 g/25 mL concentration muds.

Figure 9 shows a comparative overlay of shear stress values for the various limestone suspensions at a denoted 25 g/25 mL concentration. In freshwater, the measured shear stress values were remarkably similar for limestone Grey and limestone Castleton muds, while limestone Marl muds showed comparatively higher shear stress values. Carbonate muds prepared with saline solution shared overall similar shear stress profiles.

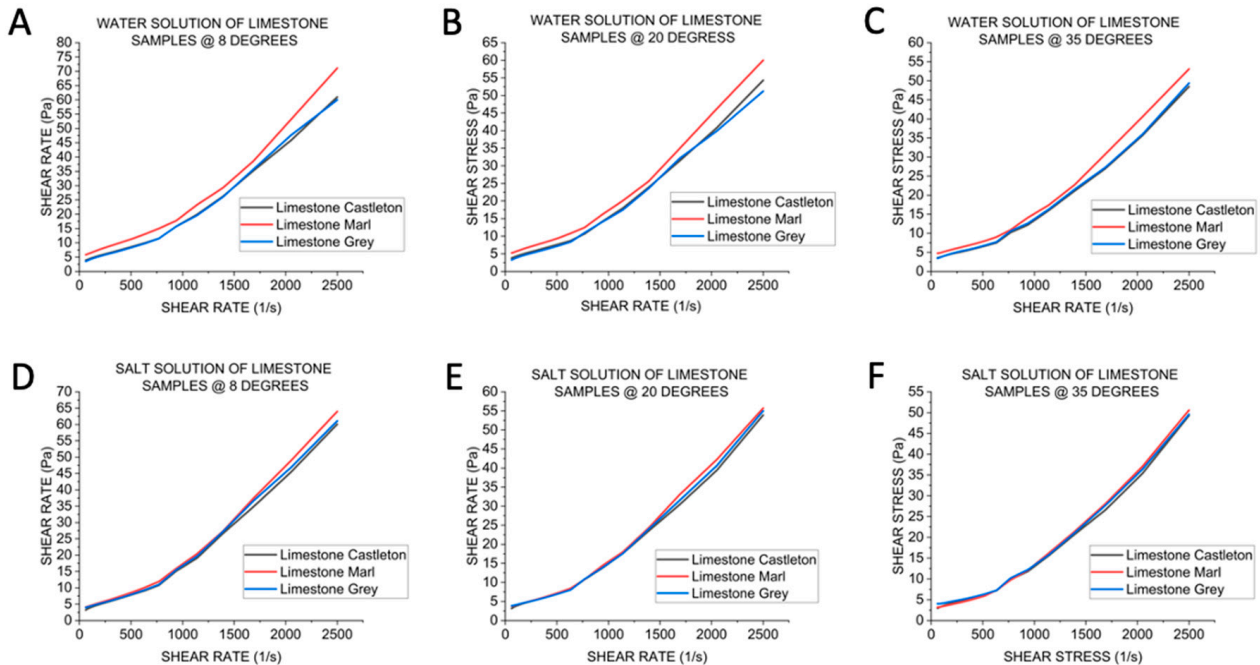


Figure 9. Influence of carbonate type on shear stress of 25 g/25 mL concentration muds.

Figure 10 shows a comparative overlay of viscosity values for the various limestone suspensions at a denoted 25 g/25 mL concentration. In freshwater, the measured viscosity values were remarkably similar for limestone Grey and limestone Castleton muds, while limestone Marl muds showed comparatively higher viscosity values. However, the model carbonate muds prepared with saline solution shared an overall similar rheology.

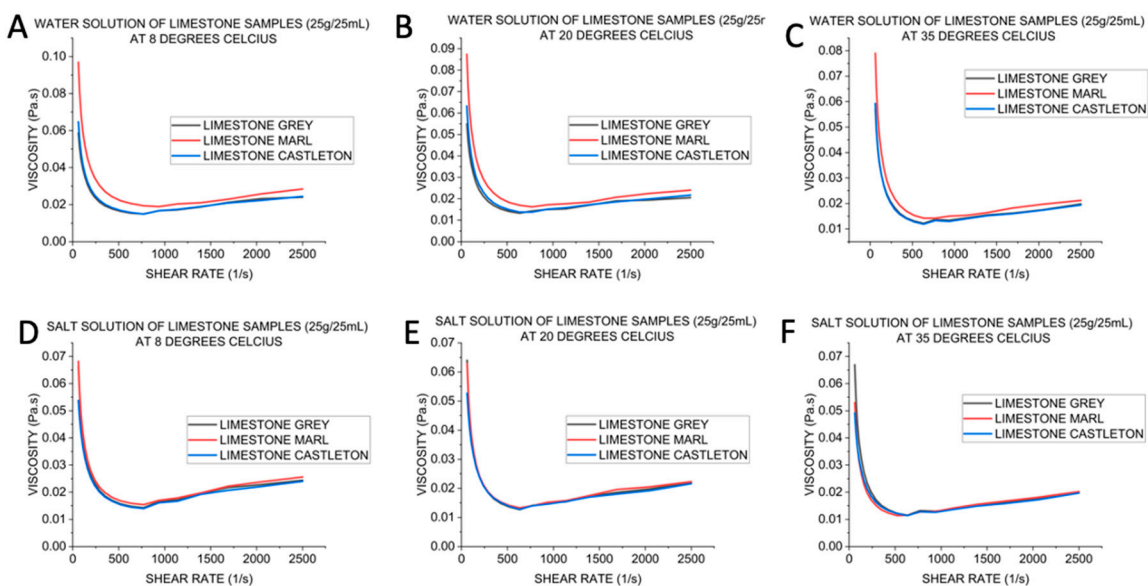


Figure 10. Influence of carbonate type on viscosity of 25 g/25 mL concentration muds.

Figure 11 shows shear stress values at various temperature conditions for limestone suspensions at a denoted 25 g/25 mL concentration. The shear stress values decreased with increasing temperature. Figure 12 shows shear viscosity values at various temperature conditions for limestone suspensions at a denoted 25 g/25 mL concentration. The mud viscosity values decreased with increasing temperature.

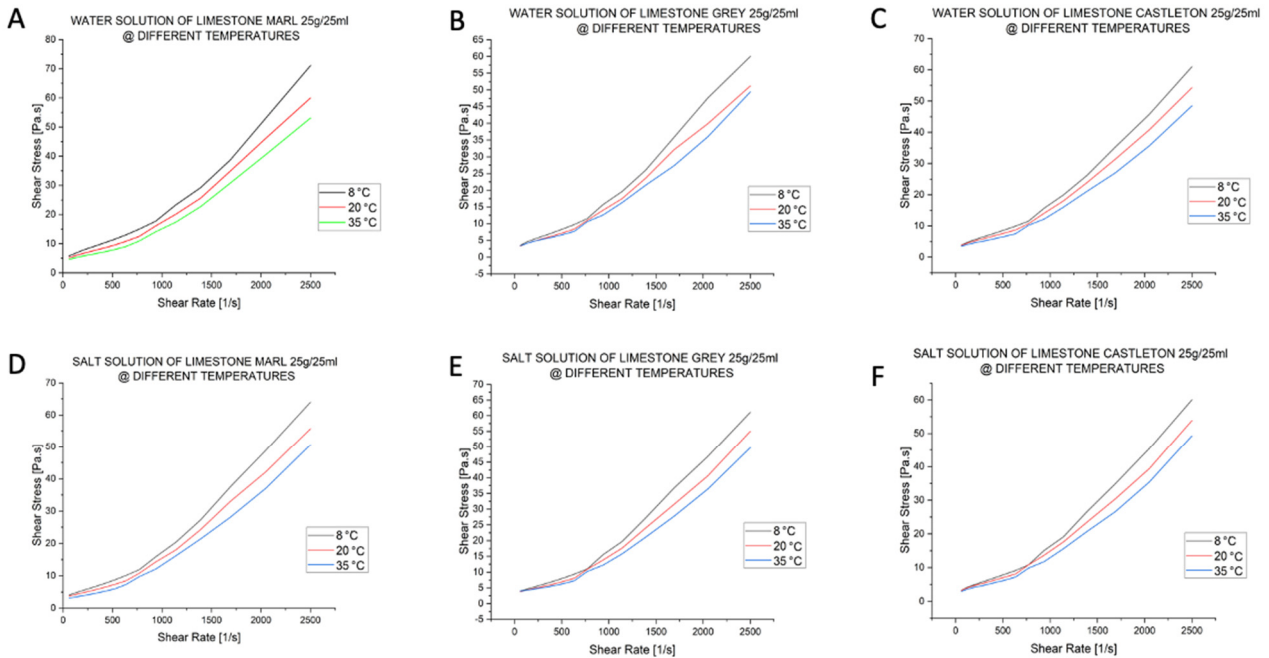


Figure 11. Influence of temperature on shear stress of 25 g/25 mL concentration muds.

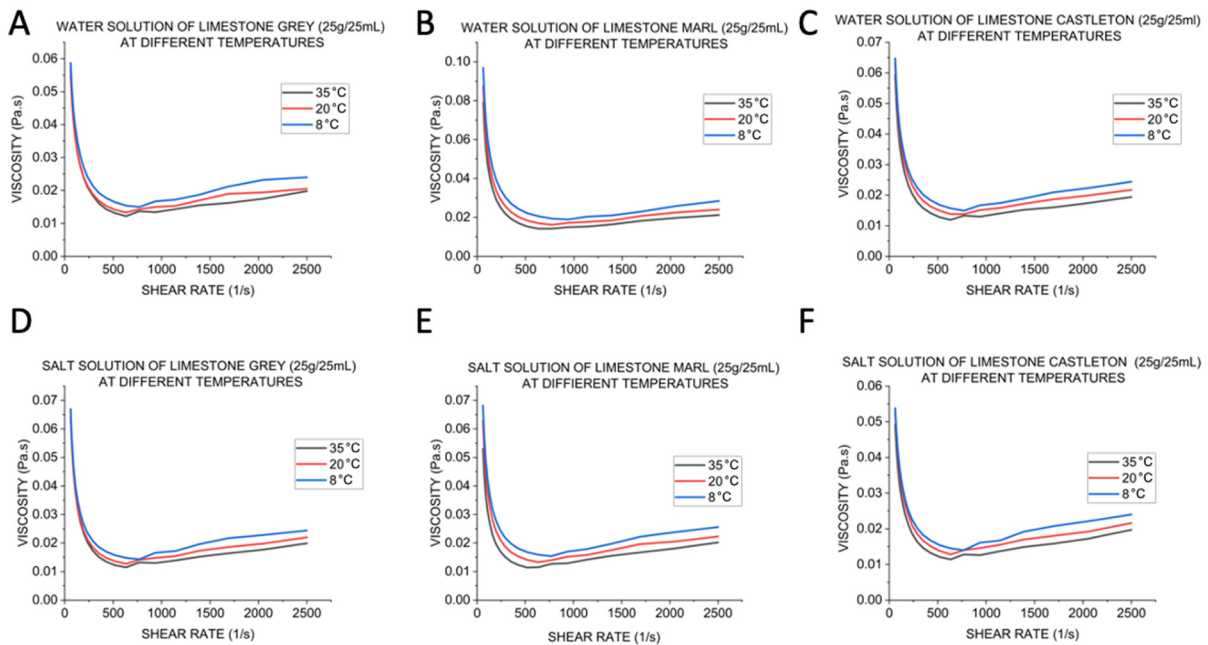


Figure 12. Influence of temperature on viscosity of 25 g/25 mL concentration muds.

3.3. Particle Size Distributions

The particle size analysis of the limestone Marl using a Mastersizer showed that 70% of the carbonate particles were below 20 μm and that 90% were below 35 μm , as shown in Figure 13. Analysis of limestone Grey showed a bimodal distribution, with 70% of the carbonate particles under 15 μm and 90% below 30 μm . Limestone Castleton analysis

revealed that 70% of the particles were below 12 μm and that 90% were below 22 μm . Overall, the particle size distributions of the limestone Grey, limestone Marl, and limestone Castleton particles were broadly comparable.

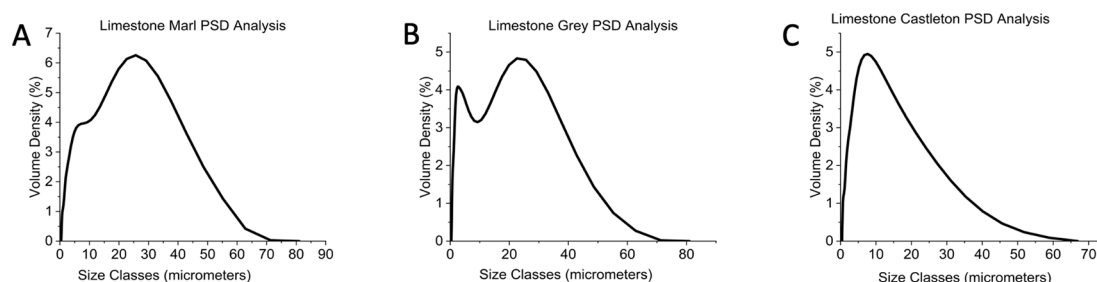


Figure 13. Particle size distributions of crushed, sieved limestone.

4. Discussion

4.1. Carbonate Mud Rheology

The current investigation deconstructs the intricate rheological nature of carbonate mud, shedding light on its behavior under diverse conditions. The measured rheology of the model carbonate muds is consistent with pseudoplasticity and weak shear thickening. Pseudoplasticity occurs at low shear rates, and shear thickening occurs at high shear rates. The model carbonate mud viscosity decreases with increasing temperature, in accordance with a reduction in viscosity of the continuous aqueous phase.

Previous studies confirmed that pseudoplasticity and weak shear thickening occur in limestone suspensions with particle sizes smaller than 100 μm [9]. Other noncolloidal suspension systems, such as starch suspensions [7], also show pseudoplasticity and weak shear thickening. Hence, the rheological behavior of the model carbonate muds is broadly comparable to the overall rheology of other noncolloidal dispersions. Corroboration with the rheology of similar noncolloidal limestone suspensions in the literature shows that pseudoplasticity is caused by shear-driven disaggregation of particle clusters [9]. The pseudoplastic regime entirely disappears when limestone suspensions are dosed with effective polymeric dispersants [9], and viscosity values at low shear rates decrease upon chemical dispersion of particles. The disappearance of the pseudoplastic regime is accompanied by extension of the shear thickening regime to lower shear rates [9], corroborating the low critical shear rate for the onset of shear thickening in noncolloidal particle suspensions. The presence of carbonate particles elevates the viscosity of carbonate mud in comparison to the viscosity of the aqueous phase. In the semi-dilute particle concentration regime, the lowest recorded carbonate mud viscosity values were approximately 2.5 times greater than the viscosity of water, as shown in the viscosity plots in Figure 2, obtained with a particle volume fraction of 1.81 percent. Experimentally measured relative viscosity values of approximately 2.5 confirm a substantial viscosifying role of occluded water in the model carbonate mud, as fully dispersed polydisperse particles are consistent with relative viscosity values of ~ 1.05 . A similar comparison of relative viscosity values in the shear-thickening regime confirms a substantial viscosifying role of occluded water in the carbonate mud. The comparison of relative viscosities provides corroborative evidence of aggregation occurring among carbonate particles in the mud, supporting evidence in the literature [9].

An elevated mud viscosity corresponds to a decreased Reynolds number, defined as the ratio of inertial to viscous forces. The reduction in Reynolds number is insufficient to preclude the occurrence of inertially driven secondary flows, such as Taylor vortices, or, alternatively, inertially driven transition flows within the measuring geometry. Viscosity measurements in the shear-thickening regime coincide with the occurrence of inertially driven secondary flows, such as Taylor vortices, or, alternatively, inertially driven transition flows. The observed linear increases in viscosity with respect to applied shear rate are not solely attributable to an innate shear-thickening rheology of the carbonate mud dispersions.

Instead, the observed linear increases in viscosity with respect to shear rate likely reflect a combined effect of innate shear-thickening rheology and the occurrence of inertially driven secondary flows, such as Taylor vortices, or, alternatively, inertially driven transition flows. Recorded minimum viscosity values on rheological plots do not necessarily demarcate a shear thickening onset. Instead, recorded minimum viscosity values may demarcate the onset of inertially driven flow artifacts. In concentric cylinder measuring geometries, the onset of inertially driven flow artifacts is often manifested as an abrupt deviation in the viscosity curve with respect to shear rate, as demonstrated in the case of aqueous biopolymeric systems not subject to shear-thickening phenomena [10]. Shear thickening in semi-dilute noncolloidal dispersions is characterized by a more gradual onset of viscosity increases at increasing shear rates, as demonstrated for corn starch suspensions. Linear viscosity increases with respect to shear rate occur in limestone particle suspensions with similar properties and characteristics to the carbonate muds used in the current investigation [9,11], lending credence to the observational validity of linear viscosity increases with respect to shear rate, as shown in Figures 2, 4, 6, 8, 10 and 12.

4.2. Influence of Particle Size Distributions

The particle sizes of the three model carbonate muds were broadly comparable. The noncolloidal carbonate particles in the model carbonate muds were primarily smaller than 62.5 μm . The measured particle size distributions showed only minor disparities among the three mineral types of limestone Grey, limestone Marl, and limestone Castleton.

Rheological experiments performed using the carbonate muds containing salt were revealing with respect to the influence of particle size distribution on the rheological behavior. The results shown in Figure 4D–F and Figure 10D–F represent conditions where electroosmotic repulsions and electroviscous effects are mostly shielded by the presence of salt. Differences in surface electric charge density among the mineral types are effectively negated in the results shown in Figure 4D–F and Figure 10D–F. Close inspection of the rheological results reveals similar viscosity curves for the three different mineral types. The observed consistency in rheological response under saline conditions for the three mineral types is illuminating. The consistent rheology for the three mineral types arose in both the semi-dilute particle concentration regime and in the concentrated particle regime. It is logical to conclude that minor disparities in the particle size distributions of the limestone Grey, limestone Marl, and limestone Castleton were not the primary cause of the differing rheological behavior of the freshwater muds prepared with the three different mineral types and that other surface phenomena, unrelated to particle size and shape, were responsible for the dissimilar rheology.

To summarize, it is recognized that the three types of carbonate particles have comparable particle size distributions, based on the particle size analysis performed using the Mastersizer. It is further observed that minor disparities in particle size distribution among the three types of carbonate particles did not substantially influence the rheology of the model carbonate mud. The empirical evidence that saline mud suspensions exhibit similar rheological curves for different minerals while freshwater mud suspensions exhibit different rheological curves for different minerals indicates that surface electric charge density accounts for the observed differences in rheology among the different carbonate minerals.

4.3. Surface Charges

Differences in observed rheological behavior among the different types of carbonate mud, especially for freshwater suspensions, are ascribed to differences in surface electric charge density and concomitant electroviscous effects. Carbonate particles in contact with an aqueous solution often carry surface electric charges, forming an electric double layer that extends into the aqueous phase. The net surface electric charge density depends on the concentration of potential determining ions (PDIs) and the composition, arrangement, coordination, and hydration of the surface atoms. Potential determining ions for limestone particle suspensions include calcium, carbonate, and magnesium [12]. Various factors and

parameters influence the concentration of potential determining ions in calcium carbonate dispersions, such as carbon dioxide saturation level, ionic strength, temperature, mineral concentration, mineral type, pH, impurities, additives, etc. Measurement, modelling, and prediction of surface electric charge density in limestone dispersions involves a multitude of factors and parameters and is beyond the scope of the current investigation.

A phenomenological approach was adopted with respect to net surface electric charge density. The independent variables in the current investigation were mineral concentration, mineral type, temperature, NaCl concentration, and shear rate. The independent variables of the investigation uniquely defined and determined the net surface electric charge density. Different carbonate mineral types have distinct net surface electric charge densities in the defined temperature, salinity, and particle concentration conditions of the measurements. Different mineral types have distinct electroviscous effects. Mineral-specific electroviscous effects cause differences in the rheological response of model carbonate muds prepared with different minerals. In the current investigation, electroviscous effects were identified in the rheological behavior of the model carbonate muds. Dissimilar electroviscous effects for different minerals originate from differences in surface electric charge density.

4.4. Electroviscous Effects

Surface charges on dispersed particles often alter the fluid viscosity. The influence of surface charges on fluid viscosity defines the electroviscous effect. Fluid viscosity changes may arise from various phenomena associated with electrically charged surfaces. Primary electroviscous effects are caused by single-particle electrostatic interactions with the shear flow field. Secondary electroviscous effects are caused by pairwise interactions among the dispersed particles. Tertiary electroviscous effects arise from changes in the physical state, structure, or internal conformation of the particles [13].

Primary electroviscous effects arise for charged particles dispersed in shearing fields. Primary electroviscous effects do not involve interparticle interactions and are accounted for in the first-order term of the virial expansion equation of viscosity [14]. Hydrodynamic flow fields in the electric double layer are distorted by electrostatic stresses exerted by the charged surface on oppositely charged fluid elements in the electric double layer. The flow field perturbation increases energy dissipation and viscosity. The primary electroviscous effect occurs at all finite particle concentrations in aqueous solutions, including dilute, semi-dilute, concentrated, packed, and ultra-packed particle concentration regimes.

Secondary electroviscous effects involve interactions between charged particle pairs. Upon the approach of two charged particles in a shearing field, electric double layers overlap and an electroosmotic repulsive force arises between the two particles. Both approaching particles deviate from their original paths. The relative interparticle velocity decreases due to the repulsive interparticle force. A difference in velocity develops between each particle and its respective local fluid environment, giving rise to an increase in energy dissipation and viscosity [15]. Secondary electroviscous effects involve interparticle interactions that are prevalent at high particle concentrations. Secondary electroviscous effects occur in semi-dilute and concentrated particle regimes. Because of the prevalence of interparticle interactions in concentrated suspensions, secondary electroviscous effects are stronger in a concentrated particle regime. In shearing fields, the relative prevalence of interparticle contacts is proportional to the square of the particle concentration. Because of the reduced prevalence of interparticle contacts in semi-dilute particle suspensions, weaker secondary electroviscous effects are observed in semi-dilute suspensions.

Electroviscous effects are stronger for smaller particles than for larger particles, due to increased specific volumetric interfacial areas and lower mean separation distances for smaller particles compared to larger particles. Electroviscous effects increase the effective volume fraction of particles in a dispersion, which is attributed to the electric double layer. The increase in the effective particle volume fraction is proportional to the specific volumetric interfacial area. Hence, smaller particles, having larger specific volumetric interfacial areas, exhibit stronger electroviscous effects than larger particles. At similar

volume fractions, smaller particles also have shorter mean separation distances than larger particles. Electric double-layer overlap is more extensive for smaller particles in comparison to larger particles, due to the shorter mean separation distance for smaller particles in comparison to larger particles. Weak electric double-layer interactions can extend over several Debye lengths, such that the separation distance effect can be quite pronounced for smaller particles. Due to the combined effect of higher specific interfacial areas and shorter mean interparticle separation distances, smaller particles have stronger electroviscous effects than larger particles [16]. Thus, electroviscous effects are typically quite weak in noncolloidal suspensions because of the relatively large particle dimensions. Nevertheless, electroviscous effects are observable in noncolloidal suspensions containing polydisperse particle sizes, with the smallest particle fraction providing a substantial surface area for electrostatic and electroosmotic interactions.

4.5. Electrolyte Effects

The thickness of the electric double layer is determined by the dielectric constant and the ionic strength of the aqueous phase. The thickness of the electric double layer determines the intensity of electroviscous effects as quantified by changes in the effective particle volume fraction attributable to electroosmotic and electrostatic interactions. The Debye–Hückel screening length defines the characteristic length scale of decay of the electric potential from the surface to the bulk solution. The Debye–Hückel screening length varies as the inverse square root of the ionic strength. The Debye–Hückel screening length decreases with increasing ionic strength. Addition of electrolytes screens charges in the electric double layer, compressing the thickness of the electric double layer. The intensity of primary and secondary electroviscous effects diminishes upon electrolyte addition [14,15].

In the context of comparing rheological data obtained for compositionally analogous saline and freshwater dispersions, it is evident that the viscosifying effect of NaCl on the continuous aqueous phase is small. Large differences in viscosity between saline and freshwater mud samples are ascribed primarily to electroviscous effects. Electroviscous effects may be quantified as an excess viscosity defined as the difference in viscosity attributable to electroviscous effects, as is evident in the concentrated particle regimes of the limestone Marl and limestone Castleton muds with and without added salt, as shown in Figure 8. For limestone Marl, differences in mud viscosities with and without added salt are quite evident.

In the semi-dilute regime, weak electroviscous effects were overshadowed by the viscosifying effect of NaCl on the continuous aqueous phase. Electroviscous effects were mostly absent in the limestone Grey muds, indicating that the pH value of the limestone Grey suspensions was close to the isoelectric point. The observed trends in electroviscous effects are consistent with a unifying principle that dissimilar surface electric charge densities exist on the various mineral particles used. The magnitude of the surface electric charge density increases with the following sequential progression in mineral types: limestone Grey, limestone Castleton, and limestone Marl.

The unifying progression in surface electric charge density for various mineral types was evident in the freshwater and saline mud viscosity values, as shown in Figure 10, with a comparison of mineral types in the concentrated particle regime. The limestone Marl muds had higher viscosities than the limestone Castleton and limestone Grey muds.

The unifying progression in surface electric charge density for various mineral types is confirmed by comparing freshwater and saline mud viscosities for identical minerals, as shown in Figure 8. Limestone Marl has the largest magnitude of electroviscous effects, followed by limestone Castleton, which has a smaller magnitude of electroviscous effects. For the limestone Grey muds, viscosity curves for freshwater and saline muds are similar. Electroviscous effects are not evident for limestone Grey muds.

4.6. Shearing Effects

At increasing shear rates, the strength of electrostatic forces remains bounded, while shear forces remain unbounded. High shear rates compress the electric double layer, and the intensity of primary and secondary electroviscous effects diminishes at increasing shear rates [16,17]. The decay in excess viscosity at high shear rates is therefore a characteristic and defining feature of electroviscous effects. The difference profile in viscosity between freshwater and saline muds, as a function of shear rate, can be used to identify electroviscous effects on rheograms. Figure 8 shows shearing effects for limestone Marl muds in the concentrated particle regime. Electroviscous effects are intense at low shear rates and decay at high shear rates. At a shear rate of 60 s^{-1} , electroviscous effects increase mud viscosity by a substantial proportion. At a shear rate of 2500 s^{-1} , electroviscous effects increase viscosity by a much smaller proportion. Figure 8 also shows the shearing effects for the limestone Castleton muds in the concentrated particle regime. The electroviscous effects are evident at low shear rates and decay at high shear rates. At a shear rate of 60 s^{-1} , electroviscous effects increase mud viscosity by a substantial proportion. At an applied shear rate of 2500 s^{-1} , electroviscous effects are indistinguishable from other effects.

For the limestone Castleton muds, ascertaining electroviscous effects on rheograms is more involved than for the limestone Marl muds. For limestone Castleton, it is evident with respect to Figure 8 that saline muds have a slightly higher bulk continuous-phase viscosity than freshwater muds. The saline mud viscosity is artificially elevated by the slightly higher bulk continuous phase. At high shear rates, in Figure 8, for limestone Castleton, the slight viscosity increase caused by salt viscosification is almost exactly balanced out by viscosity reductions caused by electrolyte shielding of electroviscous effects. At moderate shear rates for limestone Castleton muds, electroviscous effects are directly evident in Figure 8, manifested by lower viscosities for the saline limestone Castleton muds in comparison to the freshwater limestone Castleton muds. In other words, despite an ostensibly small difference in the viscosity curves in Figure 8 for saline and freshwater limestone Castleton muds, the innate electroviscous effects are somewhat stronger than is evident from the difference in the viscosity curves, due to a partial shadowing of electroviscous effects by a slight counteracting bulk-phase salt viscosification effect.

4.7. Delineating Rheological Mechanisms

The effective volume fraction approximation is an instructive means to understand and delineate the influence of multiple rheological mechanisms in the context of measured suspension viscosity. For suspensions in the dilute and semi-dilute particle concentration regimes, suspension viscosity increased mildly with increasing effective volume fraction. However, in the concentrated, packed, and densely packed particle concentration regimes, viscosity increased strongly with increasing effective volume fractions. Quantitatively, the first derivative of viscosity with respect to effective solid volume fraction was small in the dilute and semi-dilute particle concentration regimes. In the concentrated regime, the first derivative of viscosity with respect to the effective solid volume fraction was relatively large.

The incremental increase in the effective solid volume fraction ascribed to electroviscous effects can be considered a small, albeit finite perturbation. The effective solid phase volume fraction, $\phi_{s,e}$, is expressed as follows:

$$\phi_{s,e} = \phi_s + (\Delta\phi)_e \quad (1)$$

The incremental increase in viscosity ascribed to electroviscous effects is quantified as follows:

$$\mu_{s,e} = \mu_s + (\Delta\mu)_e \quad (2)$$

where ϕ denotes the solid volume fraction, ϕ_s denotes the solid volume fraction of the suspension, $\phi_{s,e}$ denotes the effective solid volume fraction of the suspension, and $(\Delta\phi)_e$ denotes the incremental increase in the effective solid volume fraction ascribed to elec-

troviscous effects. μ denotes viscosity, μ_s denotes suspension viscosity in the absence of electroviscous effects, $\mu_{s,e}$ denotes suspension viscosity with electroviscous effects, and $(\Delta\mu)_e$ denotes the incremental increase in viscosity ascribed to electroviscous effects.

A first-order Taylor expansion reveals the incremental viscosity difference ascribed to electroviscous effects, applicable for any viscosity correlation. The incremental viscosity increase ascribed to electroviscous effects is approximated as the product of two factors: the incremental increase in the effective solid-phase volume fraction ascribed to electroviscous effects and the first-order derivative of viscosity with respect to the solid volume fraction:

$$(\Delta\mu)_e \approx (\Delta\phi)_e \cdot \left. \frac{\partial\mu(\phi)}{\partial\phi} \right|_{\phi=\phi_s} \quad (3)$$

Because electroviscous effects are both interfacial and rheological effects, the incremental increase in the effective solid volume fraction ascribed to electroviscous effects is assumed to be proportional to the specific volumetric interfacial area. The specific volumetric interfacial area scales linearly with the solid-phase volume fraction. Hence, the incremental increase in the effective solid volume fraction is proportional to the solid fraction.

$$(\Delta\phi)_e = k_a(\phi_s) \quad (4)$$

The factors are combined as follows:

$$(\Delta\mu)_e \approx \overbrace{k_a(\phi_s)}^{\text{"A"}} \cdot \overbrace{\left. \frac{\partial\mu(\phi)}{\partial\phi} \right|_{\phi=\phi_s}}^{\text{"B"}} \quad (5)$$

Factor "A" and factor "B" in Equation (5) are both functions of the solid volume fraction of the suspension. Factor "A" is a linear function of the solid volume fraction. Factor "B" is a strong function of the solid volume fraction. The two distinct factors, "A" and "B", in Equation (5) together constitute a strong function of the solid-phase volume fraction of the suspension. The semi-dilute and concentrated particle suspensions used in the current investigation have solid-phase volume fractions of 1.81 percent and 26.95 volume percent, respectively. Equation (5) shows that the viscosity increase ascribed to electroviscous effects is a strong function of the solid-phase volume fraction. The large difference in the solid-phase volume fraction between the semi-dilute and concentrated muds, amplified by a strong solid volume fraction dependency in Equation (5), results in negligibly small electroviscous effects for semi-dilute muds and substantial electroviscous effects for concentrated muds.

For the semi-dilute limestone suspensions used in the current research investigation, the negligible electroviscous effects resulted in an overshadowing of electroviscous effects by the weak viscosification of the bulk aqueous phase caused by salt addition.

For the concentrated limestone suspensions used in the current investigation, strong electroviscous effects overshadow or counteract a weak viscosification of the bulk aqueous phase when salt is added to the bulk aqueous phase.

5. Conclusions

Carbonate muds show pseudoplasticity at low shear rates and weak shear thickening at high shear rates. Viscosity values measured for model carbonate muds are consistent with an aggregated particle state, in agreement with findings reported in the literature. Pseudoplasticity in carbonate mud is ascribed to shear-driven breakup and dispersal of particle aggregates. Shear thickening in carbonate muds is ascribed to hydrocluster formation.

Electroviscous effects are distinctly observable in carbonate muds. The magnitude of electroviscous effects is determined by the surface electric charge density of the carbonate mineral. Carbonate mineral types that carry net surface charges in aqueous solutions show measurable electroviscous effects. Carbonate minerals that lack surface charges in aqueous

solutions do not show substantial electroviscous effects. Electroviscous effects decrease at increasing shear rates, in agreement with theoretical considerations. Electroosmotic and electrostatic interactions are bounded in strength and are overcome by strong, unbounded viscous forces at high shear rates. Electrolytes shield electroosmotic repulsions and compress the electric double layer, reducing electroviscous effects. Electrolytes reduce the viscosity of muds containing particles with charged surfaces.

The rheological measurements performed in the current investigation are consistent with a high concentration of electrically charged particles on the surface of limestone Marl and a low concentration of charged particles on the surface of limestone Castleton. Surface charges are not rheologically evident on limestone Grey.

In rheological modeling, electroviscous effects may be quantified with the formalism of effective particle volume fractions. As a corollary, water occluded in particle aggregates contributes to the effective particle volume fraction of a suspension. Electroviscous effects also increase the effective particle volume fraction of a suspension, resulting in an increase in viscosity. Electroviscous effects are reduced by electrolyte screening and shear-induced compression of the electric double layer. These phenomena are quantifiable as reductions in effective particle volume fractions, providing a theoretically qualified modeling route to account for interparticle interactions in the context of suspension rheological models [18]. A quantitative description of electroviscous effects [19] is enabled over the entire shear rate regime.

Author Contributions: Conceptualization, W.A.M. and M.F.; Data curation, W.A.M.; Formal analysis, W.A.M., M.F. and K.G.P.; Investigation, W.A.M. and M.F.; Methodology, W.A.M., M.F. and K.G.P.; Project administration, M.F.; Resources, M.F.; Software, W.A.M.; Supervision, M.F. and K.G.P.; Validation, W.A.M., M.F. and K.G.P.; Visualization, W.A.M. and M.F.; Writing—original draft, W.A.M. and M.F.; Writing—review and editing, M.F. and K.G.P. All authors have read and agreed to the published version of the manuscript.

Funding: This research was funded by the Ghana National Petroleum Corporation (GNPC), grant number GNPC01012023.

Data Availability Statement: The datasets presented in this article are not readily available due to technical limitations.

Conflicts of Interest: The authors declare no conflicts of interest.

References

1. Schieber, J.; Southard, J.B.; Kissling, P.; Rossman, B.; Ginsburg, R. Experimental deposition of carbonate mud from moving suspensions: Importance of flocculation and implications for modern and ancient carbonate mud deposition. *J. Sed. Res.* **2013**, *83*, 1025–1031. [[CrossRef](#)]
2. Trower, E.J.; Lamb, M.P.; Fischer, W.W. The origin of carbonate mud. *Geophys. Res. Lett.* **2019**, *46*, 2696–2703. [[CrossRef](#)]
3. Geyman, E.C.; Wu, Z.; Nadeau, M.D.; Edmonson, S.; Turner, A.; Purkis, S.J.; Howes, B.; Dyer, B.; Ahm, A.S.C.; Yao, N.; et al. The origin of carbonate mud and implications for global climate. *Earth Planet Sci.* **2002**, *119*, 45. [[CrossRef](#)] [[PubMed](#)]
4. Alince, B.; Lepoutre, P. Flow behavior of pigment blend. *Tappi J.* **1983**, *66*, 57–60.
5. Senapati, P.K.; Panda, D.; Parida, A. Predicting viscosity of limestone–water slurry. *J. Miner. Mater. Charact. Eng.* **2009**, *8*, 203. [[CrossRef](#)]
6. Cheng, X.; McCoy, J.H.; Israelachvili, J.N.; Cohen, I. Imaging the microscopic structure of shear thinning and thickening colloidal suspensions. *Science* **2011**, *333*, 1276–1279. [[CrossRef](#)] [[PubMed](#)]
7. Crawford, N.C.; Popp, L.B.; Johns, K.E.; Caire, L.M.; Peterson, B.N.; Liberatore, M.W. Shear thickening of corn starch suspensions: Does concentration matter? *J. Colloid Interface Sci.* **2013**, *396*, 83–89. [[CrossRef](#)] [[PubMed](#)]
8. Barnes, H.A. Shear-thickening (“Dilatancy”) in suspensions of nonaggregating solid particles dispersed in Newtonian liquids. *J. Rheol.* **1989**, *33*, 329–366. [[CrossRef](#)]
9. He, M.; Wang, Y.; Forssberg, E. Parameter studies on the rheology of limestone slurries. *Int. J. Miner. Process.* **2006**, *78*, 63–77. [[CrossRef](#)]
10. Sveistrup, M.; van Mastrigt, F.; Norrman, J.; Picchioni, F.; Paso, K. Viability of biopolymers for enhanced oil recovery. *J. Dispers. Sci. Technol.* **2016**, *37*, 1160–1169. [[CrossRef](#)]
11. He, M.; Wang, Y.; Forssberg, E. Parameter effects on wet ultrafine grinding of limestone through slurry rheology in a stirred media mill. *Powder Technol.* **2006**, *161*, 10–21. [[CrossRef](#)]

12. Alroudhan, A.; Vinogradov, J.; Jackson, M.D. Zeta potential of intact natural limestone: Impact of potential-determining ions Ca, Mg and SO₄. *Colloids Surf. A Physicochem. Eng. Asp.* **2016**, *493*, 83–98. [[CrossRef](#)]
13. Li, J.; Cheng, Y.; Chen, X.; Zheng, S. Impact of electroviscous effect on viscosity in developing highly concentrated protein formulations: Lessons from non-protein charged colloids. *Int. J. Pharm. X* **2019**, *1*, 100002. [[CrossRef](#)] [[PubMed](#)]
14. Watterson, I.G.; White, L.R. Primary electroviscous effect in suspensions of charged spherical particles. *J. Chem. Soc. Faraday Trans. 2 Mol. Chem. Phys.* **1981**, *77*, 1115–1128. [[CrossRef](#)]
15. Blachford, J. Theory of the secondary electroviscous effect for nonidentical particles. *J. Phys. Chem.* **1969**, *73*, 3512–3513. [[CrossRef](#)]
16. Zhou, Z.; Scales, P.J.; Boger, D.V. Chemical and physical control of the rheology of concentrated metal oxide suspensions. *Chem. Eng. Sci.* **2001**, *56*, 2901–2920. [[CrossRef](#)]
17. Conceição, S.I.; Olhero, S.; Velho, J.L.; Ferreira, J.M.F. Influence of shear intensity during slip preparation on rheological characteristics of calcium carbonate suspensions. *Ceram. Int.* **2003**, *29*, 365–370. [[CrossRef](#)]
18. Pal, R. New generalized viscosity model for non-colloidal suspensions and emulsions. *Fluids* **2020**, *5*, 150. [[CrossRef](#)]
19. Rubio-Hernández, F.J. Electroviscous Effects in Stationary Solid Phase Suspensions. *Fluids* **2021**, *6*, 69. [[CrossRef](#)]

Disclaimer/Publisher’s Note: The statements, opinions and data contained in all publications are solely those of the individual author(s) and contributor(s) and not of MDPI and/or the editor(s). MDPI and/or the editor(s) disclaim responsibility for any injury to people or property resulting from any ideas, methods, instructions or products referred to in the content.